Journal of Materials Chemistry B

REVIEW

Check for updates

Cite this: J. Mater. Chem. B, 2018, 6, 2960

Investigations on the elasticity of functional gold nanoparticles using single-molecule force spectroscopy†

Li Sun, [ab] René Riedel,[c] Stefan G. Stanciu, [d] Fang Yang,*[bce] Norbert Hampp,[c] Li Xu *[a] and Aiguo Wu *[bce]

Received 25th December 2017,
Accepted 3rd April 2018

DOI: 10.1039/c7tb03309e

rsc.li/materials-b

A wide range of investigation tools and frameworks aimed at the in depth understanding of the physicochemical properties of different nanomaterials and at exploring their cellular interactions and effects have been reported in the past couple of decades. Among these, Single-Molecule Force Spectroscopy (SMFS) emerges as a very important tool for characterizing nanoparticles (NPs) and one of its very valuable applications consists in the quantitative analysis of the NPs' elasticity. In SMFS experiments that tackle this subject, a sharp tip present on the apex of a cantilever is indented into a single NP, and then the Young's modulus is determined as a measure of its elasticity, which is one of the fundamental mechanical parameters affecting the structural and functional cellular parameters. Based on such approaches, SMFS enables the observation and analysis of significant cellular effects that are relevant to various cellular parameters. In this focused review, we turn our attention towards several approaches for detecting the elasticity of NPs, systematically summarizing the divergent elasticity values of distinct gold nanoparticles (AuNPs) with different surfaces. We carry as well a critical discussion on the elasticity assessment models and the fundamental factors that influence NP elasticity assessment by means of SMFS.

1. Introduction

With the rapid progress and development of nanotechnology, a wide variety of new generation materials have emerged enabling novel cutting-edge applications in multiple critical fields, including nanomedicine[1,2] or nanoelectronics.[3,4] In this context, nanostructured and nanometer-sized materials have drawn the attention of numerous scientists because of their unique physicochemical properties and great promise in the development of applied science. Currently, nanoparticles (NPs) stand at the forefront of the rapidly developing field of nanotechnology. They serve as important components in modern nanotechnology approaches that address diverse fields and offer unprecedented opportunities to design and develop novel materials useful for various applications, *e.g.*, electrical devices,[5–7] solar cells,[8,9] imaging[10–13] or biomedical therapy.[14–18] Over the past few years, a particular focus of attention has been placed on the development of NPs that can be functionalized to exhibit distinct physicochemical properties and on their translation to biomedical research and practice.[19] In fact, given the thriving research and industrial interest in the field, the emergence of functional NPs serves as a key factor in addressing unsolved scientific and technical problems, including those involving our daily lives or those concerning biomedical and clinical applications. With respect to the latter, an important aspect that needs to be taken into account consists of the fact that functional NPs may pose a risk to human health.[20–22] Therefore, each new class of NPs must be evaluated for its potential health hazards with complex biological assays before their functionalized variants can be safely translated to the biomedical realm to realize their enormous promise.[23] Hence, in parallel to the ongoing efforts placed towards developing and synthesizing novel NPs that take place at a very rapid pace, simultaneously, their properties should be investigated using complementary chemical and physical approaches that allow their in-depth understanding. Among the different types of NPs that have lately drawn major

[a] College of Science, Nanjing Forestry University, Nanjing, Jiangsu, P. R. China. E-mail: xuliqby@njfu.edu.cn
[b] CAS Key Laboratory of Magnetic Materials and Devices & Key Laboratory of Additive Manufacturing Materials of Zhejiang Province & Division of Functional Materials and Nanodevices, Ningbo Institute of Materials Technology and Engineering, Chinese Academy of Sciences, Ningbo, P. R. China. E-mail: yangf@nimte.ac.cn, aiguo@nimte.ac.cn
[c] Fachbereich Chemie, Philipps Universität Marburg, Marburg, Germany
[d] Center for Microscopy-Microanalysis and Information Processing, University Politehnica of Bucharest, Bucharest, Romania
[e] Cixi Institute of BioMedical Engineering, Ningbo Institute of Materials Technology and Engineering, Chinese Academy of Sciences, Ningbo, P. R. China

† Electronic supplementary information (ESI) available. See DOI: 10.1039/c7tb03309e

interest, gold nanoparticles (AuNPs) represent maybe the most extensively studied class of NPs and a focal point of the scientific community, not only because of their unique optical properties[24,25] but also because of their excellent mechanical properties.[26,27] The field of gold nanoparticle research has attracted huge interest over the past years. There are many important review papers that focus on gold nanoparticles uptake[28] and their effect on cellular processes,[29] their various roles in therapeutics and diagnostics scenarios,[22,30–32] toxicology aspects,[22,33,34] or sensing.[35–44] Studies that address their synthesis[45–50] or various physicochemical properties, such as plasmon resonances,[51] spin polarization[52] or fluorescence quenching[53] are also important, as they provide in a concise manner insights into specific aspects important for key fields of science. Review papers that focus on the mechanical properties of gold nanomaterials are few in number, and mainly address very specific topics, *e.g.* ref. 54–56. To the best of our knowledge no review paper to summarize the current level of knowledge and available assessment methodologies for gold nanoparticle elasticity has been reported to date. However, the more general topic of the mechanical properties of nanoparticles has been addressed in the insightful review article authored by Guo *et al.*,[57] where the authors discuss important aspects such as hardness, elastic modulus, adhesion and friction. To better understand AuNPs, thorough studies on their mechanical properties are necessary. In particular, the properties of special interest include elasticity and adhesion. Elasticity, the ability of a material to resist an applied deforming force and to return to its original size and shape when the force is removed, is typically used for describing the mechanical properties of a material, as is adhesion, which is defined as a tendency to keep the substances together in close contact. With respect to nanoscale entities such as AuNPs, specific mechanical properties play a significant role in related studies and applications.[58] In order to obtain a clear picture on the importance of the addressed topic, we have performed a literature survey of the research articles published between 2008 and 2018. The methodology for this survey was as follows: we have queried the Web of Knowledge database (Clarivate Analytics, USA) to retrieve articles, proceedings papers and meeting abstracts whose title include the terms ''Gold'' or ''Au'' and ''mechanical''. This search yielded a total of 269 results, of which 89 (~33%) represent studies addressing directly the mechanical properties (or having deep implications for) various nanoscale or nanostructured gold-based advanced materials such as nanocages,[59] nanosprings,[60] nanorods,[61,62] nanolines,[63] nanoparticles,[64,65] thin films,[54,66] nanoporous Au,[67,68] *etc.* We have also performed a more narrow query, retrieving the same item types, published within the same time frame, using combinations of the terms ''Au'' or ''Gold'' and ''elasticity'', ''stiffness'', ''hardness''. This second query yielded a total of 46 publications, of which 15 (~33%) directly addressed nanoscale gold structures, *e.g.* ref. 69–72.

In many regards, including mechanical ones, AuNPs exhibit completely different properties in comparison to bulk gold. For instance, depending on their composition, size, shape and ligands, small AuNPs can exceed the elasticity of pure bulk gold (78 GPa).[69,73] Ramos *et al.* measured an elastic modulus of 100 GPa for six-fold icosahedron AuNPs with a size of 22 nm.[74] An accurate quantitative understanding of their elasticity and adhesion properties is important for improving the design of functional AuNPs and modelling their cellular uptake or their intercellular trafficking, which are complex processes and not yet well understood. Investigations on such topics can be however quite difficult to perform mainly because there are many factors that influence the uptake or trafficking mechanisms, including size, shape and chemical conjugation. Among these factors, the size of the NPs plays a particularly important role. For example, Trono *et al.* showed that the uptake of a certain amount of 20 nm AuNPs is faster than that of the same amount of smaller (10 nm) or larger (30 nm, 40 nm, 50 nm and 100 nm) AuNPs of the same shape.[75] Smaller NPs undergo faster exocytosis, whereas larger NPs seem to bind to fewer different proteins.[76] It is also important to consider the agglomeration of NPs since this may lead to inferior uptake ratios. In addition to size, the NP shape has an effect on the uptake mechanism. Wang *et al.* investigated the uptake of polyethylene glycol (PEG)-coated AuNPs with different shapes by breast cancer cells (MDS-MB-435)[77] and found nanohexapod AuNPs exhibit a higher uptake ratio than nanorods and nanocage AuNPs. Chan *et al.* determined that spherical AuNPs have a higher uptake ratio than gold nanorods when the NPs are uncoated.[78] When coated with ligands, gold nanorods were found to be internalized faster than gold nanospheres, which is probably because of the higher concentration of ligands per NP that interact with the cell surface. The interaction between the NPs and cell surfaces is one of the important factors that control the uptake mechanism. Because the cell surface is negatively charged, a NP with a positively charged surface may seem to be taken up more readily than a NP with a negatively charged surface.[79–81] However, the complexity of the surrounding media leads to a NP–protein corona which controls the NP–cell-interaction.[82–85] This corona depends on the medium and its properties, such as pH value. Furthermore, the uptake ratio has also been shown to be highly dependent on cell type.

To date, the effect of the mechanical properties of NPs, such as adhesion and elasticity, on cellular uptake has rarely been investigated. However, there are some publications that quantitatively analyze how the elasticity and adhesion of different AuNPs influence their biological effects. Tao *et al.* revealed that macrophages are not able to phagocytose very soft samples.[86] Moreover, the phagocytosis of soft NPs can be constrained by particle deformation.[87] Hence, soft, flexible particles are expected to have longer blood circulation lifetimes than hard particles. Yi *et al.* established a theoretical model to describe the influence of elasticity on particle wrapping.[88] According to this model, softer particles are less prone to wrapping than stiffer ones, which can be ascribed to the difference in elastic energy. A stiffer particle is rapidly encompassed by a membrane, whereas a soft particle would initially rub along the membrane's surface. Total wrapping around a soft particle would take more time. Thus, more energy is required for the wrapping, making it less likely to happen. This could be one of the reasons why PEGylated

AuNPs are less prone to be taken up by cells than bare AuNPs. These studies provide important evidence that when it comes to cellular investigations, the mechanical properties of NPs influence their interaction with cells. Therefore, understanding how to quantitatively measure NPs' elasticity, and defining optimal protocols in this regard, will be helpful for appropriately collecting information that is extremely valuable for their efficient translation to biological applications.

Over the last several decades, atomic force microscopy-based single molecule force spectroscopy (SMFS) has evolved into a universal and useful tool for the study of the interactions and the binding forces between individual molecules, providing more physical information about the nano-/micro-size samples.[89] Such high-resolution techniques capable of addressing single-molecules are now widely used for measuring the behavior of a molecule under pressing, stretching or torsional mechanical forces. A great deal has been learned recently from various advanced approaches based on SMFS, such as triggering of enzymatic activities,[90] in-depth understanding of polysaccharides,[91] information about protein folding and unfolding,[92] bacteriorhodopsin folding, or insights into cell adhesion.[93] Through its flexibility, SMFS breaks through the limitations imposed by very specific measuring conditions, which apply in the case of other techniques, and allows even precise measurements in liquids of single NPs. Because in the frame of a SMFS measurement the cantilever may touch different areas on the surface of the NP, there are different measuring approaches and results. In this review, we discuss the average elasticity for series of AuNPs based on significant statistic calculations.

When applied as a single-molecule force spectroscopy (SMFS) technique, atomic force microscopy (AFM) serves as an optimal tool for detecting elasticity because of the reduced number of limitations referring to the measuring conditions. It has thus become one of the most frequently employed methods to measure the elasticity of a cell.[94,95] AFM based SMFS[89] overcomes previous limitations by enabling precise observations on elasticity over a nanoscale area and can probe samples exhibiting diverse physical properties, *e.g.* conductive or non-conductive, stiff or soft, and flat or rough samples.[96,97] Because of this flexibility, it serves not only as a universal method for the external characterization of materials but also as a useful tool for understanding various biological aspects.[98,99] For example, several studies have demonstrated the use of SMFS in the single-molecule characterization of protein unfolding, whereby the adhesion property of a DNA string[100] and the binding force of a polymer to a substrate have been investigated.[101] As highlighted also above, as a parameter of primary importance, elasticity also serves as a key factor in completely understanding the physical properties of an NP that influence its cellular uptake and toxicity.[19,88] Recently, a novel qualitative method was demonstrated for the distinction between stiff NPs and soft NPs. Soft zwitterionic nanogels were found capable to pass more rapidly/easily through physiological barriers, *i.e.*, splenic filtration, than their stiffer counterparts, preventing splenic accumulation and extending their circulation half-life.[102] However, SMFS is yet to be regarded as a default tool or method to provide the accurate quantitative calculation and analysis of elasticity, a role that we consider that SMFS in conjunction with a nanoindentation model can successfully assume in the not so distant future. The interested readers can find additional information on the working principles of AFM and SMFS in the ESI.†

2. Approaches to measure the elasticity of NPs

The quantitative understanding of the mechanical properties of NPs represents a key factor for their smooth integration into important biomedical applications (and not only). Importantly, in the context of a quantitative measurement of a material's stiffness, elasticity is referred to as Young's modulus. Normally, the Young's modulus is dependent on the change in indentation, which is likely to be affected by the low-bending stiffness of the linear nanostructure at the terminal end. Because of the different apices of probes, the appropriate model can be used as a description of elasticity, *e.g.*, spherical, linear and conical models. First, the Hertz model considers a linearly elastic sphere indenting an elastic surface without surface forces or adhesion. In this situation, the Hertzian equation leads to a final calculation of elasticity that depends on the loading force, Poisson's ratio, the radius of the indenter and the indentation depth. Second, the Derjaguin–Muller–Toporov (DMT) model is used for an elastic sphere with a rigid surface but includes the van der Waals force outside the contact region. Normally, it is applicable to stiff samples with low adhesion. Third, Sneddon's equation considers a rigid conical shape on an elastic half-space. In the Sneddon model, the equation is related to the loading force, Poisson's ratio, half of the indenter and the indentation depth. For instance, a conical tip with a tiny diameter has been utilized for analyzing the elasticity of a series of AuNPs.[103] SMFS is performed over the same areas to measure the mechanical response of the NPs during the approach and the retraction of the AFM probe, as shown in Scheme 1. In particular, the elasticity is extracted from the approach process. The response curve is presented in Scheme 2, as well as the corresponding situation of the tip. Owing to the conical apex on the top of the cantilever, the elasticity will be calculated from the deflection *versus* distance data. The deflection sensitivity of the SMFS, which relates to the output voltage corresponding to the applied force, is assessed and adjusted during measurement (to preserve the calibration) through the force–distance profiles on the surface of the NPs. The interested readers can find details as well as a comparison with the advanced peakforce quantitative nanomechanical property mapping method (QNM) in the ESI.†

The Young's modulus of the NPs is influenced by the outer organic molecules, with thicker polymer coatings resulting in stiffer colloids, and by the type of polymer coatings (*e.g.*, cross-linked *versus* non-cross-linked).[104] Because the outer polymer packing density can induce stiff protection of the core, particularly under aqueous conditions, the Young's modulus in water E_w is stiffer than that in air E_a.[103] For instance, the behaviour of PEG plays a determining role with respect to

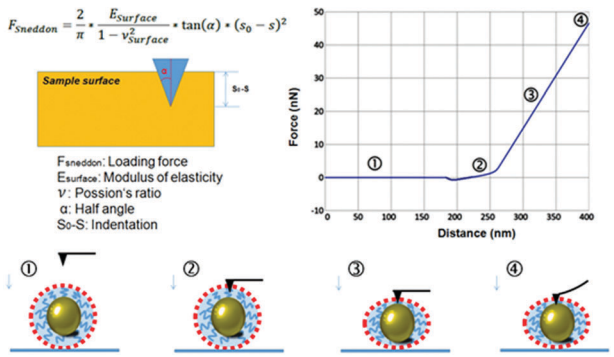

Scheme 1 Conical cantilever indented into a single AuNP. The force curve of indentation from SMFS is dependent on the process. ① A cantilever approaches the NP, and the force remains zero. ② The tip indents the polymer first, and the force increases slowly. ③ The tip indents continuously until it touches the core, and the force increases faster, which means that the slope here is greater than that in process ②. ④ The whole NP is pressed down, and the force increases to the same extent as in process ③. The stiffness is calculated according to Sneddon's equation. Copyright 2016 Wiley.[103]

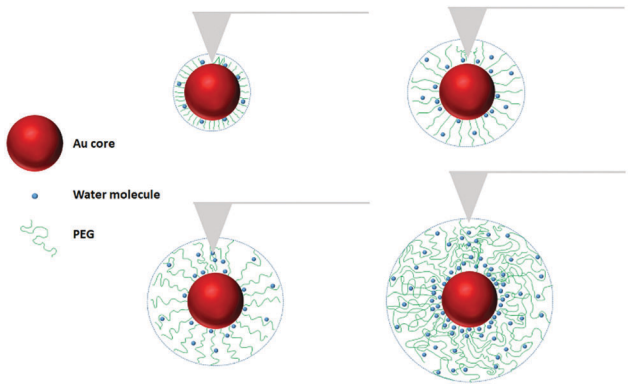

Scheme 2 Depiction of a conical tip intending into a single NP in water. Water molecules are trapped by the PEG ligands.

the elasticity of PEGylated surfaces. The situation where water molecules are trapped in the PEG ligands, as shown in Scheme 2, is especially of interest, as it leads to E_w values that are significantly larger than the equivalent values in air E_a.[103]

3. AuNPs conjugated with different PEG derivatives

3.1 Imaging of AuNPs conjugated with different PEG derivatives

A critical aspect of biological applications consists in the cellular internalization of NPs, which is affected by their mechanical properties and cell surface mechanics.[105,106] Despite the considerable progress in investigating the intrinsic properties of NPs, the role of elasticity has not been scientifically summarized yet. To quantitatively explain the correlation between the elasticity and biological effects, a homogenous library of PEGylated AuNPs was synthesized.[103] The AuNPs were successfully prepared and characterized by scanning electron

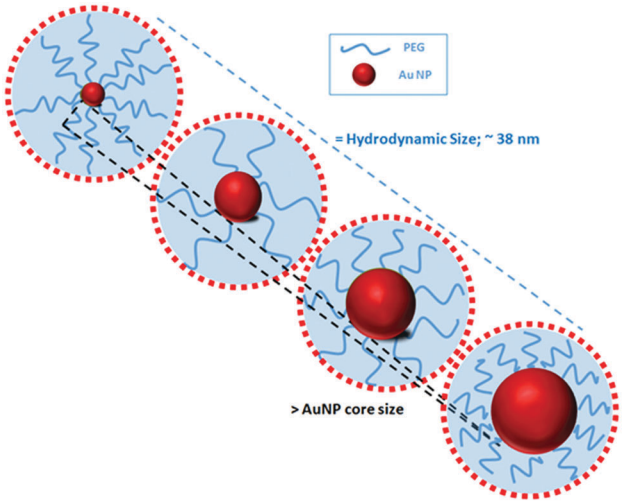

Scheme 3 Different AuNPs with the same hydrodynamic size are obtained by coating them with different PEG derivatives. The hydrodynamic size is *ca.* 38 nm.

microscopy (SEM) and AFM. Alternatively, AuNPs with different core sizes and different PEG coatings but with the same hydrodynamic size (see Scheme 3) were synthesized in order to demonstrate the strong dependence of their physicochemical properties on the thickness of the polymer on the substrates.

The experimental procedure and results reported in an important previous work[107] referring to AuNPs for stiffness assessment will be presented below: all the solutions were diluted 10 times to avoid aggregation and then were dropped onto a 1 × 1 cm piece of stainless steel with a smooth surface (roughness *ca.* 1 nm). All stainless steel patches were cleaned with acetone and chloroform and then dried at 18 °C under vacuum. After dropping, it was necessary to wait 20–30 minutes until the NPs sank to the bottom of the substrate. To image and locate the NPs on the substrate, the measurements (see Fig. 1) were performed using a JEOL JSM-7500F high resolution SEM equipped with a backscattered electron detector ($Y_1Si_2O_7$:Ce^{3+}; yttrium aluminium garnet activated by Ce^{3+}, Autrata, Czech Republic).

Considering that interactions with the water content in PEG can influence the measurements of stiffness, all the samples were measured in water and after vacuum exposure (the water content was less than 2%). After the submersion process, all the samples in water could be measured directly using an AFM. For the measurements performed after vacuum exposure, all the samples were dried naturally for 8 hours till the water disappeared to ensure that the NPs were dispersed on the substrate. After treatment under vacuum for 1 hour, the samples were immediately measured with the AFM. This process was followed step by step due to water interference. A multi-mode IV AFM (Veeco, Santa Barbara, CA) was chosen for the measurements. The topological images (see Fig. 2) were obtained in tapping mode (TM) with constant amplitude attenuation. The cantilever approach (silicon-tip on a nitride lever, $k = 0.32$ N m^{-1}, f = 40–75 kHz) was utilized with an initial drive amplitude of 0.499 V (tip oscillation amplitude of 1.5 V).

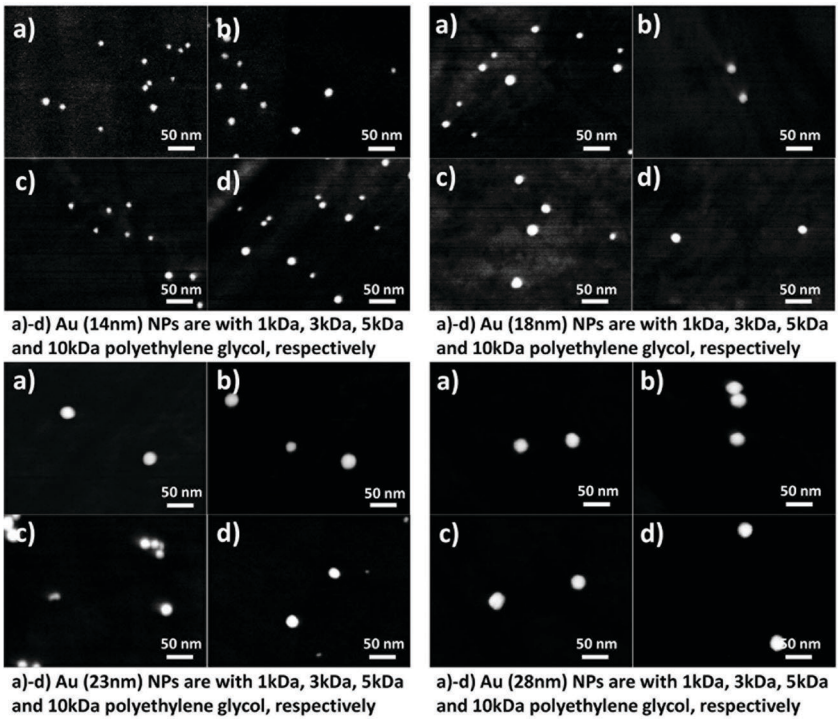

Fig. 1 Selected AFM topological images of PEGylated AuNPs. The scale bar corresponds to 50 nm.

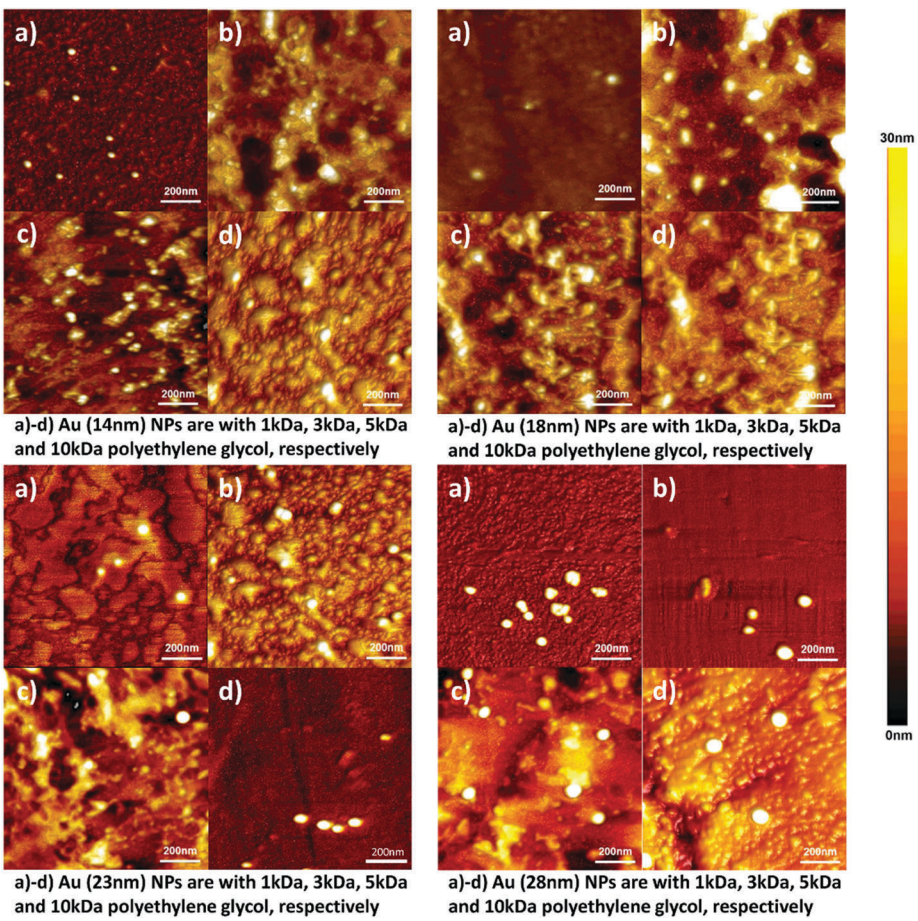

Fig. 2 Selected AFM topological images of PEGylated AuNPs. The scale bar corresponds to 200 nm.

3.2 Elasticity of AuNPs conjugated with different PEG derivatives in air and in water

In a previous landmark experiment,[107] the indentation behavior of the surface terminated with AuNPs–PMA–PEG was reflected, and the curves of the single force *versus* distance of the cantilever were recorded at the same time. Thus, Young's Modulus could be calculated by analyzing the approach process (see Scheme 1). A calibration procedure was performed to analyze the exact area of the conical tip, which was subsequently used for all measurements. Each NP was approached approximately 60 times, and more than 15 NPs located on different areas on the substrate were measured. Therefore, for each set of samples, more than 900 curves were obtained and processed using the NanoScope Analysis 1.5 software.

All trace curves were quantitatively calculated for indentation, which is related to the equation of Young's modulus. Young's modulus is dependent on the tip radius, the deflection sensitivity, the spring constant, the tip half angle and Poisson's ratio. Because of the conical shape of the tip, Sneddon's equation was selected for analyzing the stiffness of the AuNPs. The results, including plots and 3D heat maps of the Young's modulus and size for the experiments conducted in vacuum and in water, are presented in Fig. 3 and 4. In addition, because of the massive statistical calculations depicted in Fig. 3(b) and 4(b) the Gaussian distribution for each measurement and the average values calibrated from all experimental data are shown in Fig. 3(a) and 4(a), respectively. The plots show that the Young's modulus is related to the size of the NPs and the molecular weight of PEG. Moreover, the Young's modulus increases when the core size of NPs with same molecular weight of PEG increases. The same situation happens as well when the molecular weight of PEG of NPs with same core size increases. In addition, the elasticity of the AuNPs in water was observed to be almost two orders of magnitude higher than that in vacuum. This result revealed that the water content in PEG plays an important role in the hardness of the NPs because of the cross-linking of the PEG ligands *via* their interactions with water molecules. It was thus demonstrated that the NPs in water are harder than those in vacuum. From a statistical point of view, the NPs in water have a larger hydrodynamic size than those in vacuum, allowing the tip to touch a larger effective area of the NPs based on the analysis of statistic calculations (see Scheme 4).

4. AuNPs conjugated with different proteins

Quantitative studies on the elastic properties of a material are also important for understanding and predicting its resistance to permanent deformation, as well as for modifying the design of functional materials and structures.[108] Some studies have

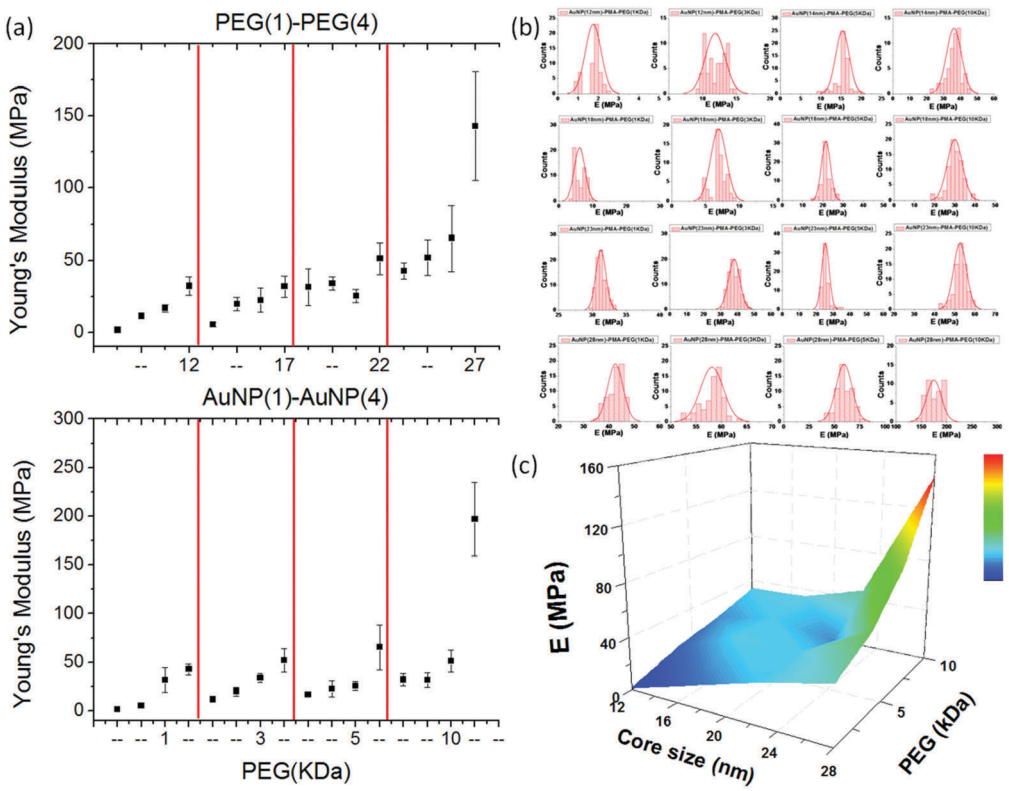

Fig. 3 (a) Plots showing the Young's modulus of all the AuNPs. All the measurements were conducted in air. (b) Plots of the Young's modulus of all the AuNPs. All the measurements were conducted in water. (c) 3D heat-map of the Young's modulus. Specifically, the 3D heat-map of the Young's modulus in air (modulus of elasticity, *E*) *versus* the core size and the molecular weight of PEG is plotted. Copyright 2016 Wiley.[103]

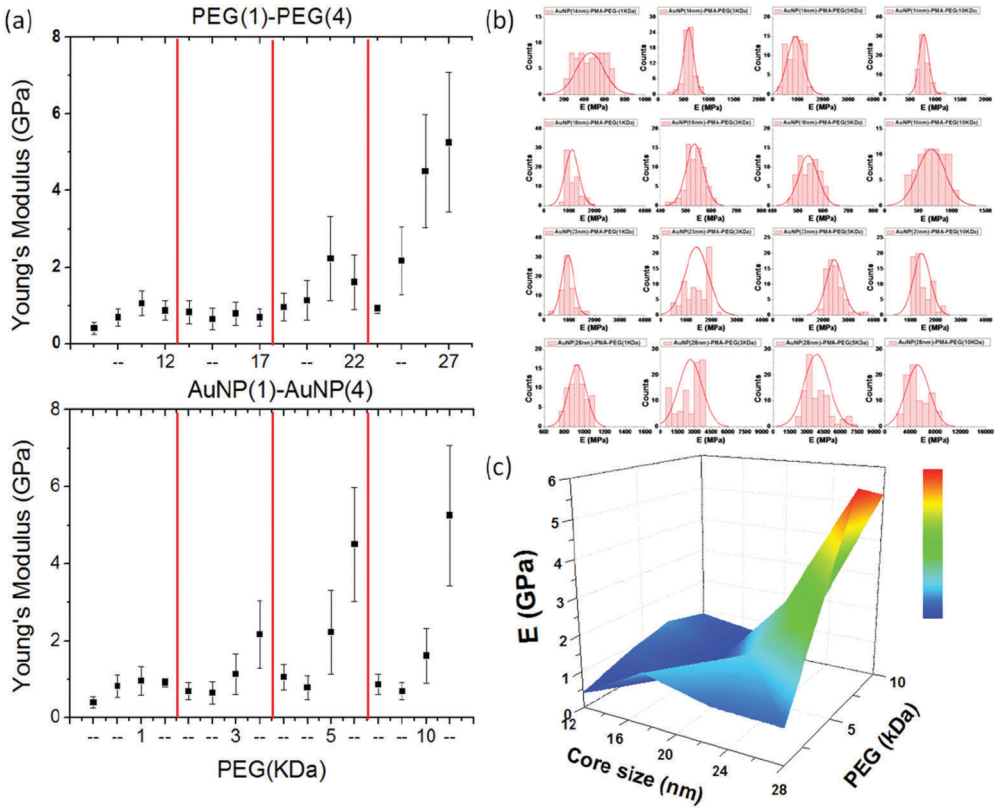

Fig. 4 (a) Stiffness measurements in water. The Gaussian distribution of the Young's modulus in water is plotted. (b) Stiffness measurements in air. The Gaussian distribution of the Young's modulus in air is plotted. (c) 3D heat-map of the Young's modulus. Specifically, the 3D heat-map of the Young's modulus in water (modulus of elasticity, *E*) *versus* the core size and molecular weight of PEG is plotted. Copyright 2016 Wiley.[103]

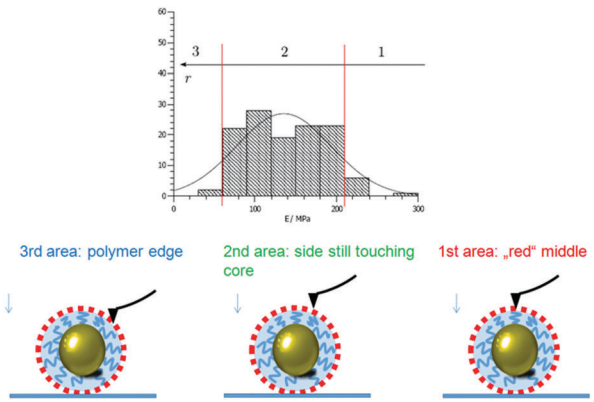

Scheme 4 Tip touching different positions on the AuNP.

stated that the elasticity depends on the size of the nanoscale object under investigation and its biomolecule (*e.g.*, protein) coating.[109–111] In this case, the resistance of a material to deformation is a way to quantitatively measure the stiffness of the material and can be used for optimizing the morphology and composition towards further biological research and application. Functional NPs conjugated with proteins are considered biocompatible and biodegradable carriers for biological applications, as this type of NP was proven to have low toxicity.[112] Moreover, NPs decorated with chitosan on their surface were reported to respond to pH in a controllable drug-release system[113] and exerted an outstanding cytotoxic effect against cancer cells and in nude mice.[114] NPs with targeting molecules have been used as a marker for radiotherapy.[115] In fact, with the rapidly increasing demand in the biological and medical fields, investigation of the mechanical properties of NPs will help scientists better understand their intrinsic characteristic, thereby enabling them to explore more fundamental and highly promising applications. In this regard, Wampler *et al.*[116] demonstrated the elasticity of AuNPs whose surface was modified with bovine serum albumin (BSA) and streptavidin, as shown in Fig. 5.[116]

Their investigation utilized an analytical method to explore the elasticity of the nanosized AuNPs coated with proteins, which has garnered considerable interest regarding the evaluations of the stiffness of functionalized NPs. The goal of such studies is to incorporate the findings into fabricating modified nanomaterials for biomedical applications that take advantage of their unique mechanical properties. In summary, we overviewed the recent progress on the elasticity assessment of modified AuNPs with a core size diameter of 10–20 nm based on nanoindentation by SMFS. According to the measured values of the Young's modulus, the smaller particles are stiffer and more resistant to protein deformation than their larger counterparts. The results of this study can be used for tuning the properties of AuNPs with surfaces functionalized by proteins.

	Reduced modulus (GPa)	Yang's modulus (GPa)	Hardness (GPa)
Clean	55.27±7.68	46.43±7.68	1.64±0.29
ODT	14.69±3.04	12.34±3.04	0.82±0.23
Set 1			
Au conjugated BSA (BSA-NP) 10 nm	1.55±0.57	1.30±0.57	0.12±0.06
Au	2.30±0.28	1.93±0.28	0.28±0.04
BSA	1.46±0.53	1.23±0.53	0.10±0.01
Au conjugated BSA (BSA-NP) 20 nm	1.48±0.57	1.24±0.57	0.08±0.03
Au	1.38±0.17	1.16±0.17	0.17±0.02
BSA	1.49±0.61	1.25±0.61	0.07±0.01
Set 2			
Biotin labeled BSA	9.88±1.80	8.30±1.80	0.64±0.21
Au conjugated streptavidin (STV-NP) 10 nm	11.28±7.57	9.48±7.75	0.22±0.09
Au	15.63±7.59	13.13±7.59	0.28±0.06
Streptavidin	5.69±1.17	4.78±1.17	0.13±0.03
Au conjugated streptavidin (STV-NP) 20 nm	1.21±0.26	1.02±0.26	0.13±0.06
Au	1.34±0.24	1.13±0.24	0.17±0.03
Streptavidin	1.01±0.12	0.85±0.12	0.07±0.01

Fig. 5 Values of the reduced modulus, Young's modulus and hardness of various AuNPs conjugated with different proteins. Copyright 2009 Elsevier.[116]

sample	thickness *t* (nm)	Y_D (GPa)	Y_C (GPa)
31A	31±<1	4.0	3.9
41A	41±2	3.5	3.6
41B	41±2	2.7	3.2
41C	41±2	3.9	4.9
44A	44±1	3.0	3.4
44B	44±1	3.2	4.0
60A	60±1	(4.3)[α]	4.4
60B	60±1	3.7	5.0

[α]The Y_D value extracted for sample 60A was not further considered as it might be affected by substrate tilt changes.

Fig. 6 Elastic and viscoelastic properties of covalently cross-linked AuNPs (*i.e.*, 1,9-nonanedithiol cross-linked AuNPs with a 3.8 nm core diameter) in films of different thicknesses. The membrane thickness and biaxial moduli determined for the AuNP membranes analysed in this study were obtained using the peak-deflection method (Y_D) and the circular fit method (Y_C). Copyright 2014 American Chemical Society.[129]

5. Cross-linked AuNPs

NP networks hold as well enormous potential when considering the development of next-generation electrical devices. Previous studies showed that the elasticity of supercrystals and thin films based on different non-cross-linked NPs is dependent on the size of the capping ligands and packing density as well as orientation order.[117] In addition, the strength of the outer chemical bonds in the coating of the nanocrystals also plays a significant role, as does the strength of the interparticle interaction between the ligands.[118] A freestanding monolayer of dodecanethiol-capped AuNPs with high ordering has been shown to exhibit a much smaller elasticity than highly ordered cross-linked AuNPs,[119–121] which is due to the strong particle–particle interactions. Therefore, a covalently cross-linked structure will increase the elastic modulus. Cross-linked AuNPs have been used as transduction elements for fabricating resistive strain gauges,[122–125] pressure sensors,[126,127] and chemiresistors,[128] wherein the transduction mechanism is based on the distance between NPs because of force-induced strain or sorption-induced swelling. Obviously, the performance of sensors and flexible electronics based on NPs with different shapes and modified molecules is dependent on their mechanical properties, such as elasticity and adhesion. In previous experiments the elasticity has been successfully measured by calculating the nanoindentation and force deflection using SMFS. For example, Vossmeyer *et al.*[129] demonstrated that AFM bulge tests are well suited to probe the elastic properties of a cross-linked AuNP-film shown in Fig. 6,[129] which has applications in flexible electronics, actuators, and sensors.[121] Furthermore, based on a nanoindentation approach, the elastic properties of the membranes were investigated by analyzing their pressure dependence on deflection, leading to a calculated Young's modulus of *ca.* 2 GPa.[121] In other studies, the elastic modulus of the membranes consisting of non-cross-linked dodecanethiol AuNPs was found to be *ca.* 0.025 GPa.[130] Conversely, in other experiments the elastic modulus of the disordered nonanedithiol interlinked AuNP-film was found to be *ca.* 5 GPa, which is on the same order of magnitude as those reported for colloidal crystals and highly ordered monolayers of dodecanethiol-stabilized AuNPs.[119,131] The results of these investigations will contribute to further study of the stiffness

of cross-linked AuNPs and its impact towards their efficient translation to reliable real-life applications.

6. Discussion and conclusions

Investigating the elasticity aspects of distinct AuNPs with various coatings and sizes and in different environments has gained massive interest over the past years mainly because the use of AuNPs in daily life applications as well as in biomedical research and practice is increasing in a very rapid pace. The great versatility of AuNPs with different characteristics (coatings, sizes, or mechanical properties) offers great potential for a wide range of disciplines. However, with respect to many aspects their mechanical properties have still not been fully comprehended, which causes concern as less understood aspects can have a negative impact on their reliability and function. Considerable progress has been made in the past couple of decades in our understanding of mechanical properties such as elasticity. The elasticity of NPs serves as an important parameter with respect to critical aspects of drug delivery or bioreporters, such as cellular uptake or induced mechanical properties. Understanding the effects of the elasticity of NPs on their biological behaviour is essential for the development of novel nanodrugs and biomedical materials. In particular the stiffness of the outer coatings of NPs is crucial to predict and control the ability of the NPs to diffuse and disperse inside cells or the human body. Obtaining information about how to improve their accumulation time in tissues, circulation lifetime in the blood and resistance to metabolism is an important task for further applications in the biomedical field. In the case of electrical devices, the mechanical properties (*i.e.* elasticity) of underlying materials such as AuNPs, hold deep implications for the performance and reliability of the fabricated electronics and electronic components. This is dependent on the orientation order, enabling strong interparticle interaction between face-to-face oriented neighboring crystal lattices, which is attributed to the structure or array of AuNPs.

In this review, we have surveyed a series of recent approaches for elastic modulus measurements of the stiffness applicable to different types of AuNPs. These approaches demonstrate that the elasticity of the AuNPs can be successfully studied by SMFS and analyzed by complementary computational methods, enhancing their further implementation in next-gen nanomedicine applications or nanodevices with applicability in various other fields. Important conclusions that can be drawn from this review: (i) the elasticity of AuNPs in water is larger than that in air, (ii) the elasticity of AuNPs conjugated with protein is larger than that of AuNPs conjugated with small molecules, and (iii) the elasticity of cross-linked AuNPs is larger than that of non-cross-linked AuNPs. Furthermore, exploring the nanoindentation of a single AuNP will be helpful for algorithmic calculation of the modulus. This will open up many possibilities to exploit the intrinsic properties of functional designed AuNPs for future next-gen applications.

Conflicts of interest

The authors declare no conflict of interest.

Acknowledgements

This work was supported by funding of the Ningbo Institute of Industrial Technology, CAS Y20408RA11, the Zhejiang Provincial Natural Science Foundation of China GF18H180047 and the Postdoctoral scientific research Foundation of Zhejiang Province Human resources and U1432114 Aiguo Wu is grateful to the Special Program for Applied Research on Super Computation of the NSFC-Guangdong Joint Fund (the second phase) (U1501501 to Aiguo Wu), the Zhejiang Province Financial Supporting (2017C33129, 2017C03042, and LY18H180011), the Bureau of Science and Technology of Ningbo Municipality City (2015C50004, 2015B11002, and 2017C110022), CAS Innovation Team. Stefan G. Stanciu acknowledges the financial support of the Romanian Executive Agency for Higher Education, Research, Development and Innovation Funding (UEFISCDI) *via* grants PN-II-RU-TE-2014-4-1803 (MICRONANO) and PN-III-P2-2.1-PED-2016-0450 (Q-NANOBIOTIC).

References

1 M. Srikanth and J. Kessler, *Nat. Rev. Neurol.*, 2012, **8**, 307–318.
2 S. Sonkaria, S. H. Ahn and V. Khare, *Recent Pat. Food, Nutr. Agric.*, 2012, **4**, 8–18.
3 D. Akinwande, N. Petrone and J. Hone, *Nat. Commun.*, 2014, **5**, 5678.
4 X. Dong, W. Huang and P. Chen, *Nanoscale Res. Lett.*, 2011, **6**, 60.
5 R. J. Tseng, C. Tsai, L. Ma, J. Ouyang, C. S. Ozkan and Y. Yang, *Nat. Nanotechnol.*, 2006, **1**, 72.
6 G. Konstantatos and E. H. Sargent, *Nat. Nanotechnol.*, 2010, **5**, 391.
7 H. Choi, S.-J. Ko, Y. Choi, P. Joo, T. Kim, B. R. Lee, J.-W. Jung, H. J. Choi, M. Cha and J.-R. Jeong, *Nat. Photonics*, 2013, **7**, 732.
8 W. J. Beek, M. M. Wienk and R. A. Janssen, *Adv. Mater.*, 2004, **16**, 1009–1013.
9 M. A. Green, A. Ho-Baillie and H. J. Snaith, *Nat. Photonics*, 2014, **8**, 506–514.
10 Y. Jin, C. Jia, S.-W. Huang, M. O'donnell and X. Gao, *Nat. Commun.*, 2010, **1**, 41.
11 Y. I. Park, K. T. Lee, Y. D. Suh and T. Hyeon, *Chem. Soc. Rev.*, 2015, **44**, 1302–1317.
12 L. V. Wang and S. Hu, *Science*, 2012, **335**, 1458–1462.
13 L. Tarpani, D. Ruhlandt, L. Latterini, D. Haehnel, I. Gregor, J. R. Enderlein and A. I. Chizhik, *Nano Lett.*, 2016, **16**, 4312–4316.
14 E. C. Dreaden, A. M. Alkilany, X. Huang, C. J. Murphy and M. A. El-Sayed, *Chem. Soc. Rev.*, 2012, **41**, 2740–2779.

15 J. J. Giner-Casares, M. Henriksen-Lacey, M. Coronado-Puchau and L. M. Liz-Marzan, *Mater. Today*, 2016, **19**, 19–28.
16 P. D. Howes, R. Chandrawati and M. M. Stevens, *Science*, 2014, **346**, 1247390.
17 J. Ge, E. Neofytou, T. J. Cahill III, R. E. Beygui and R. N. Zare, *ACS Nano*, 2011, **6**, 227–233.
18 K. McNamara and S. A. Tofail, *Adv. Phys.*, 2017, **2**, 54–88.
19 P. Rivera-Gil, D. Jimenez de Aberasturi, V. Wulf, B. Pelaz, P. del Pino, Y. Zhao, J. M. de la Fuente, I. Ruiz de Larramendi, T. Rojo, X. J. Liang and W. J. Parak, *Acc. Chem. Res.*, 2013, **46**, 743–749.
20 H. Krug and P. Wick, *Angew. Chem., Int. Ed.*, 2011, **50**, 1260–1278.
21 A. Elsaesser and C. V. Howard, *Adv. Drug Delivery Rev.*, 2012, **64**, 129–137.
22 M. F. H. Carneiro and F. Barbosa, *J. Toxicol. Environ. Health, Part B*, 2016, **19**, 129–148.
23 R. Mout, D. F. Moyano, S. Rana and V. M. Rotello, *Chem. Soc. Rev.*, 2012, **41**, 2539–2544.
24 X. H. Huang, P. K. Jain, I. H. El-Sayed and M. A. El-Sayed, *Lasers Med. Sci.*, 2008, **23**, 217–228.
25 S. Linic, U. Aslam, C. Boerigter and M. Morabito, *Nat. Mater.*, 2015, **14**, 567–576.
26 D. Maharaj and B. Bhushan, *Beilstein J. Nanotechnol.*, 2014, **5**, 822–836.
27 C. H. Lu, I. Donch, M. Nolte and A. Fery, *Chem. Mater.*, 2006, **18**, 6204–6210.
28 S. Ahmad, A. A. Zamry, H. T. T. Tan, K. K. Wong, J. Lim and R. Mohamud, *Mol. Immunol.*, 2017, **91**, 123–133.
29 Z. Xiang, K. J. Wang, W. Z. Zhang, S. W. Teh, A. Peli, P. L. Mok, A. Higuchi and S. S. Kumar, *J. Cluster Sci.*, 2018, **29**, 1–7.
30 M. Singh, D. C. C. Harris-Birtill, S. R. Markar, G. B. Hanna and D. S. Elson, *Nanomedicine*, 2015, **11**, 2083–2098.
31 L. A. Austin, B. Kang and M. A. El-Sayed, *Nano Today*, 2015, **10**, 542–558.
32 M. Mathiyazhakan, C. Wiraja and C. J. Xu, *Nano-Micro Lett.*, 2018, **10**, 10.
33 N. Hadrup, A. K. Sharma, M. Poulsen and E. Nielsen, *Regul. Toxicol. Pharmacol.*, 2015, **72**, 216–221.
34 G. Libralato, E. Galdiero, A. Falanga, R. Carotenuto, E. de Alteriis and M. Guida, *Molecules*, 2017, **22**, 1439.
35 M. Moskovits, *Rev. Mod. Phys.*, 1985, **57**, 783–826.
36 S. W. Zeng, K. T. Yong, I. Roy, X. Q. Dinh, X. Yu and F. Luan, *Plasmonics*, 2011, **6**, 491–506.
37 D. Vilela, M. C. Gonzalez and A. Escarpa, *Anal. Chim. Acta*, 2012, **751**, 24–43.
38 V. K. K. Upadhyayula, *Anal. Chim. Acta*, 2012, **715**, 1–18.
39 Y. C. Zhang, W. D. Chu, A. D. Foroushani, H. B. Wang, D. Li, J. Q. Liu, C. J. Barrow, X. Wang and W. R. Yang, *Materials*, 2014, **7**, 5169–5201.
40 J. Cao, T. Sun and K. T. V. Grattan, *Sens. Actuators, B*, 2014, **195**, 332–351.
41 M. Alagiri, P. Rameshkumar and A. Pandikumar, *Microchim. Acta*, 2017, **184**, 3069–3092.
42 P. A. Rasheed and N. Sandhyarani, *Microchim. Acta*, 2017, **184**, 981–1000.
43 E. Priyadarshini and N. Pradhan, *Sens. Actuators, B*, 2017, **238**, 888–902.
44 F. Zarlaida and M. Adlim, *Microchim. Acta*, 2017, **184**, 45–58.
45 M. Brust and C. J. Kiely, *Colloids Surf., A*, 2002, **202**, 175–186.
46 M. Kang, H. Lee, T. Kang and B. Kim, *J. Mater. Sci. Technol.*, 2015, **31**, 573–580.
47 P. D. Shankar, S. Shobana, I. Karuppusamy, A. Pugazhendhi, V. S. Ramkumar, S. Arvindnarayan and G. Kumar, *Enzyme Microb. Technol.*, 2016, **95**, 28–44.
48 V. S. Marangoni, J. Cancino-Bernardi and V. Zucolotto, *J. Biomed. Nanotechnol.*, 2016, **12**, 1136–1158.
49 Z. H. Farooqi, S. R. Khan, R. Begum and A. Ijaz, *Rev. Chem. Eng.*, 2016, **32**, 49–69.
50 H. Liu, J. T. Feng and W. Q. Jie, *J. Mater. Sci.: Mater. Electron.*, 2017, **28**, 16585–16597.
51 V. Amendola, R. Pilot, M. Frasconi, O. M. Marago and M. A. Iati, *J. Phys.: Condens. Matter*, 2017, **29**, 203002.
52 Y. Yamamoto and H. Hori, *Rev. Adv. Mater. Sci.*, 2006, **12**, 23–32.
53 D. Ghosh and N. Chattopadhyay, *J. Lumin.*, 2015, **160**, 223–232.
54 P. Jelinek, R. Perez, J. Ortega and F. Flores, *Phys. Rev. B: Condens. Matter Mater. Phys.*, 2008, **77**, 115447.
55 P. Velez, S. A. Dassie and E. P. M. Leiva, *Phys. Rev. B: Condens. Matter Mater. Phys.*, 2010, **81**, 235435.
56 D. Cakir and O. Gulseren, *Phys. Rev. B: Condens. Matter Mater. Phys.*, 2011, **84**, 085450.
57 D. Guo, G. X. Xie and J. B. Luo, *J. Phys. D: Appl. Phys.*, 2014, **47**, 013001.
58 C. Jiang, S. Singamaneni, E. Merrick and V. V. Tsukruk, *Nano Lett.*, 2006, **6**, 2254–2259.
59 M. A. Mahmoud, P. Szymanski and M. A. El-Sayed, *J. Phys. Chem. Lett.*, 2012, **3**, 3527–3531.
60 J. Xu, H. Wang, C. C. Liu, Y. M. Yang, T. Chen, Y. W. Wang, F. Wang, X. G. Liu, B. G. Xing and H. Y. Chen, *J. Am. Chem. Soc.*, 2010, **132**, 11920–11922.
61 Y. Gan, Z. Sun and Z. Chen, *J. Appl. Phys.*, 2015, **118**, 164304.
62 B. Reischl, A. L. Rohl, A. Kuronen and K. Nordlund, *Sci. Rep.*, 2017, **7**, 16257.
63 S. Olliges, S. Frank, P. A. Gruber, V. Auzelyte, H. Solak and R. Spolenak, *Mater. Sci. Eng., A*, 2011, **528**, 6203–6209.
64 C. Mendoza, T. Pietsch, J. S. Gutmann, D. Jehnichen, N. Gindy and A. Fahmi, *Macromolecules*, 2009, **42**, 1203–1211.
65 U. Cataldi, R. Caputo, Y. Kurylyak, G. Klein, M. Chekini, C. Umeton and T. Burgi, *J. Mater. Chem. C*, 2014, **2**, 7927–7933.
66 J. Borges, M. S. Rodrigues, T. Kubart, S. Kumar, K. Leifer, M. Evaristo, A. Cavaleiro, M. Apreutesei, R. M. S. Pereira, M. I. Vasilevskiy, T. Polcar and F. Vaz, *Thin Solid Films*, 2015, **596**, 8–17.
67 G. Pia and F. Delogu, *Chem. Phys. Lett.*, 2015, **635**, 35–39.
68 G. Pia and F. Delogu, *Acta Mater.*, 2015, **99**, 29–38.

69 Q. F. Gu, G. Krauss, W. Steurer, F. Gramm and A. Cervellino, *Phys. Rev. Lett.*, 2008, **100**, 045502.
70 C. Yan, H. Portales, N. Goubet, I. Arfaoui, S. Sirotkin, A. Mermet and M. P. Pileni, *Nanoscale*, 2013, **5**, 9523–9527.
71 B. T. Lee and J. F. Ranville, *J. Hazard. Mater.*, 2012, **213**, 434–439.
72 M. Ramos, L. Ortiz-Jordan, A. Hurtado-Macias, S. Flores, J. T. Elizalde-Galindo, C. Rocha, B. Torres, M. Zarei-Chaleshtori and R. R. Chianelli, *Materials*, 2013, **6**, 198–205.
73 C. Hanser, *Horst Kuchling: Taschenbuch der Physik*, 2011.
74 M. Ramos, L. Ortiz-Jordan, A. Hurtado-Macias, S. Flores, J. Elizalde-Galindo, C. Rocha, B. Torres, M. Zarei-Chaleshtori and R. Chianelli, *Materials*, 2013, **6**, 198–205.
75 J. Trono, K. Mizuno, N. Yusa, T. Matsukawa, K. Yokoyama and M. Uesaka, *J. Radiat. Res.*, 2011, **52**, 103–109.
76 M. Dobrovolskaia, A. Patri, J. Zheng, J. Clogston, N. Ayub, P. Aggarwal, B. Neun, J. Hall and S. McNeil, *Nanomedicine*, 2009, **5**, 106–117.
77 Y. Wang, K. Black, H. Luehmann, W. Li, Y. Zhang, X. Cai, D. Wan, S. Liu, M. Li, P. Kim, Z. Li, L. Wang, Y. Liu and Y. Xia, *ACS Nano*, 2013, **7**, 2068–2077.
78 B. Chithrani, A. Ghazani and W. Chan, *Nano Lett.*, 2006, **6**, 662–668.
79 E. Frohlich, *Int. J. Nanomed.*, 2012, **7**, 5577–5591.
80 Z. G. Yue, W. Wei, P. P. Lv, H. Yue, L. Y. Wang, Z. G. Su and G. H. Ma, *Biomacromolecules*, 2011, **12**, 2440–2446.
81 T. H. Chung, S. H. Wu, M. Yao, C. W. Lu, Y. S. Lin, Y. Hung, C. Y. Mou, Y. C. Chen and D. M. Huang, *Biomaterials*, 2007, **28**, 2959–2966.
82 L. Wang, J. Li, J. Pan, X. Jiang, Y. Ji, Y. Li, Y. Qu, Y. Zhao, X. Wu and C. Chen, *J. Am. Chem. Soc.*, 2013, **135**, 17359–17368.
83 A. Alkilany, P. Nagaria, C. Hexel, T. Shaw, C. Murphy and M. Wyatt, *Small*, 2009, **5**, 701–708.
84 A. Lesniak, F. Fenaroli, M. Monopoli, C. Aberg, K. Dawson and A. Salvati, *ACS Nano*, 2012, **6**, 5845–5857.
85 S. Conner and S. Schmid, *Nature*, 2003, **422**, 37–44.
86 S. Tao and T. Desai, *J. Controlled Release*, 2005, **109**, 127–138.
87 K. Beningo and Y. Wang, *J. Cell Sci.*, 2002, **115**, 849–856.
88 X. Yi, X. Shi and H. Gao, *Phys. Rev. Lett.*, 2011, **107**, 098101.
89 K. C. Neuman and A. Nagy, *Nat. Methods*, 2008, **5**, 491.
90 H. Gumpp, E. M. Puchner, J. L. Zimmermann, U. Gerland, H. E. Gaub and K. Blank, *Nano Lett.*, 2009, **9**, 3290–3295.
91 M. Rief, F. Oesterhelt, B. Heymann and H. E. Gaub, *Science*, 1997, **275**, 1295–1297.
92 B. Jagannathan, P. J. Elms, C. Bustamante and S. Marqusee, *Proc. Natl. Acad. Sci. U. S. A.*, 2012, **109**, 17820–17825.
93 M. Benoit, D. Gabriel, G. Gerisch and H. E. Gaub, *Nat. Cell Biol.*, 2000, **2**, 313–317.
94 A. Harris and G. Charras, *Nanotechnology*, 2011, **22**, 345102.
95 P. Carl and H. Schillers, *Pfluegers Arch.*, 2008, **457**, 551–559.
96 R. Farahi, A. Charrier, A. Tolbert, A. Lereu, A. Ragauskas, B. Davison and A. Passian, *Sci. Rep.*, 2017, **7**, 152.
97 A. Ross, Z. Jiang, M. Bastmeyer and J. Lahann, *Small*, 2012, **8**, 336–355.
98 G. Wei, Q. Li, S. Steckbeck and L. C. Ciacchi, *Phys. Chem. Chem. Phys.*, 2014, **16**, 3995–4001.
99 Q. Li, T. Zhang, Y. Pan, L. C. Ciacchi, B. Xu and G. Wei, *RSC Adv.*, 2016, **6**, 12893–12912.
100 M. Erdmann, R. David, A. Fornof and H. E. Gaub, *Nat. Nanotechnol.*, 2010, **5**, 154–159.
101 M. Geisler, B. N. Balzer and T. Hugel, *Small*, 2009, **5**, 2864–2869.
102 L. Zhang, Z. Cao, Y. Li, J. R. Ella-Menye, T. Bai and S. Jiang, *ACS Nano*, 2012, **6**, 6681–6686.
103 P. Del Pino, F. Yang, B. Pelaz, Q. Zhang, K. Kantner, R. Hartmann, N. Martinez de Baroja, M. Gallego, M. Moller, B. B. Manshian, S. J. Soenen, R. Riedel, N. Hampp and W. J. Parak, *Angew. Chem., Int. Ed.*, 2016, **55**, 5483–5487.
104 A. Skardal, J. Zhang, L. McCoard, S. Oottamasathien and G. D. Prestwich, *Adv. Mater.*, 2010, **22**, 4736–4740.
105 K. Haase and A. Pelling, *J. R. Soc., Interface*, 2015, **12**, 20140970.
106 C. Friedsam, D. Ingber, D. Weitz and O. Sahin, *Biophys. J.*, 2010, **98**, 367A–368A.
107 P. del Pino, F. Yang, B. Pelaz, Q. Zhang, K. Kantner, R. Hartmann, N. M. de Baroja, M. Gallego, M. Moller, B. B. Manshian, S. J. Soenen, R. Riedel, N. Hampp and W. J. Parak, *Angew. Chem., Int. Ed.*, 2016, **55**, 5483–5487.
108 S. Corcoran, R. Colton, E. Lilleodden and W. Gerberich, *Phys. Rev. B: Condens. Matter Mater. Phys.*, 1997, **55**, 16057–16060.
109 S. Guo, L. Hong, B. Akhremitchev and J. Simon, *Photochem. Photobiol.*, 2008, **84**, 671–678.
110 N. Kol, Y. Shi, M. Tsvitov, D. Barlam, R. Shneck, M. Kay and I. Rousso, *Biophys. J.*, 2007, **92**, 1777–1783.
111 J. Michel, I. Ivanovska, M. Gibbons, W. Klug, C. Knobler, G. Wuite and C. Schmidt, *Proc. Natl. Acad. Sci. U. S. A.*, 2006, **103**, 6184–6189.
112 A. Schrand, M. Rahman, S. Hussain, J. Schlager, D. Smith and S. Ali, *Wiley Interdiscip. Rev.: Nanomed. Nanobiotechnol.*, 2010, **2**, 544–568.
113 L. Xie, W. Tong, D. Yu, J. Xu, J. Li and C. Gao, *J. Mater. Chem.*, 2012, **22**, 6053–6060.
114 S. Bae, K. Ma, T. Kim, E. Lee, K. Oh, E. Park, K. Lee and Y. Youn, *Biomaterials*, 2012, **33**, 1536–1546.
115 Y. Huang, Y. Luo, W. Zheng and T. Chen, *ACS Appl. Mater. Interfaces*, 2014, **6**, 19217–19228.
116 H. P. Wampler and A. Ivanisevic, *Micron*, 2009, **40**, 444–448.
117 P. Podsiadlo, G. Krylova, B. Lee, K. Critchley, D. Gosztola, D. Talapin, P. Ashby and E. Shevchenko, *J. Am. Chem. Soc.*, 2010, **132**, 8953–8960.
118 J. He, P. Kanjanaboos, N. Frazer, A. Weis, X. Lin and H. Jaeger, *Small*, 2010, **6**, 1449–1456.
119 C. Yan, I. Arfaoui, N. Goubet and M. Pileni, *Adv. Funct. Mater.*, 2013, **23**, 2315–2321.
120 C. Yan, H. Portales, N. Goubet, I. Arfaoui, S. Sirotkin, A. Mermet and M. Pileni, *Nanoscale*, 2013, **5**, 9523–9527.
121 H. Schlicke, E. Leib, A. Petrov, J. Schroder and T. Vossmeyer, *J. Phys. Chem. C*, 2014, **118**, 4386–4395.

122 J. Herrmann, K. Muller, T. Reda, G. Baxter, B. Raguse, G. de Groot, R. Chai, M. Roberts and L. Wieczorek, *Appl. Phys. Lett.*, 2007, **91**, 183105.
123 T. Vossmeyer, C. Stolte, M. Ijeh, A. Kornowski and H. Weller, *Adv. Funct. Mater.*, 2008, **18**, 1611–1616.
124 C. Farcau, H. Moreira, B. Viallet, J. Grisolia, D. Ciuculescu-Pradines, C. Amiens and L. Ressier, *J. Phys. Chem. C*, 2011, **115**, 14494–14499.
125 N. Olichwer, E. Leib, A. Halfar, A. Petrov and T. Vossmeyer, *ACS Appl. Mater. Interfaces*, 2012, **4**, 6151–6161.
126 M. Segev-Bar, A. Landman, M. Nir-Shapira, G. Shuster and H. Haick, *ACS Appl. Mater. Interfaces*, 2013, **5**, 5531–5541.
127 M. Segev-Bar and H. Haick, *ACS Nano*, 2013, **7**, 8366–8378.
128 F. Ibanez and F. Zamborini, *Small*, 2012, **8**, 174–202.
129 H. Schlicke, E. W. Leib, A. Petrov, J. H. Schroder and T. Vossmeyer, *J. Phys. Chem. C*, 2014, **118**, 4386–4395.
130 N. Goubet, C. Yan, D. Polli, H. Portales, I. Arfaoui, G. Cerullo and M. Pileni, *Nano Lett.*, 2013, **13**, 504–508.
131 K. Mueggenburg, X. Lin, R. Goldsmith and H. Jaeger, *Nat. Mater.*, 2007, **6**, 656–660.